

Two Descriptions for the Photocounting Detection of Radiation Passed through a Random Medium: A Comparison for the Turbulent Atmosphere

J. Peřina and V. Peřinová

Laboratory of Optics, Palacký University, Olomouc, Czechoslovakia

M. C. Teich* and Paul Diamant

Columbia University, New York, New York 10027

(Received 20 September 1972)

Two descriptions of light passed through a random medium (the turbulent atmosphere), as recently proposed by Diamant and Teich and by Tatarski, are derived from a unified approach based on the coherent-state technique. The photon counting distributions for both descriptions are numerically compared for special states of the field (chaotic and coherent radiation and their superposition); it is found that these distributions lie very close to each other for non-vacuum-states while they precisely coincide for the Fock states.

I. INTRODUCTION

Recently, two alternate descriptions have been proposed for the statistics of light passed through an inhomogeneous random medium and particularly through the turbulent atmosphere. The first of these, proposed by Diamant and Teich,¹ uses a slightly modified form of the standard photodetection equation in order to determine the photon counting statistics; this description has been used for studies of special states of the field, such as chaotic radiation and coherent radiation, as well as their superposition, in a number of papers.¹⁻⁶ The other description has been proposed by Tatarski,⁷ who has considered second-order correlation effects for fully coherent monochromatic light (monochromatic coherent state). These restrictions have been removed by Peřina,⁸ and the Tatarski description has been extended to correlation effects of all orders for light having arbitrary statistical behavior; as a consequence, the modified photodetection equation for the photon counting statistics has been obtained.

In this last paper,⁸ it has been shown that both the Diamant and Teich and the Tatarski descriptions can be considered valid quantum mechanically; the first is based on the number operator \hat{n} in a volume V of the field at time t , while the second is based on the operator $\tilde{\nu}$, representing the number of photons crossing a surface S in the time interval $(0, T)$ (under the assumptions $S \gg \lambda^2$ and $T \gg \omega^{-1}$, where λ is the wavelength and ω is the frequency of the light). Although there are some special conditions required for the validity of each of these descriptions,⁸ for $V \equiv S(c/\sqrt{\epsilon})T$ (here c is the velocity of light in *vacuo* and ϵ is the mean permittivity of the medium) both methods might be expected to yield similar results. We discuss this point in greater detail in Sec. II by treating the propagation of light through a random medium as

a dynamic problem with the help of the coherent-state technique.^{9,10} In Sec. III, we provide a numerical comparison for the photon counting distributions calculated by means of both of these descriptions.

II. UNIFIED TREATMENT OF BOTH DESCRIPTIONS

The detailed treatment of the propagation of light through a random medium will be given elsewhere¹⁰; we restrict our discussion here to those results required for the purpose of comparing the Diamant-Teich and the Tatarski descriptions.

We describe the field through the number operator

$$\hat{n} = \int_{L^3} \hat{A}^\dagger(x) \cdot \hat{A}(x) d^3x = \sum_{\lambda} \hat{a}_{\lambda}^\dagger \hat{a}_{\lambda}, \quad (1)$$

where

$$\hat{A}(x) = L^{-3} \sum_{\vec{k}, s} \vec{e}^{(s)}(\vec{k}) \hat{a}_{\vec{k}s} e^{i(\vec{k} \cdot \vec{x} - \hbar c t)}. \quad (2)$$

Here, we allow for simplicity that the volume V coincides with the normalization volume L^3 of the field (this is, at least approximately, the case in practical realizations); $\hat{A}(x)$ is the detection operator at the space-time point $x \equiv (\vec{x}, t)$, \hat{a}_{λ} and $\hat{a}_{\lambda}^\dagger$ are the annihilation and creation operators of a photon in the mode $\lambda \equiv (\vec{k}, s)$, respectively, \vec{k} is the momentum of the photon and s is its polarization, c is velocity of light in *vacuo*, and $\vec{e}^{(s)}(\vec{k})$ is the unit polarization vector.

In the Heisenberg picture, the following equations of motion apply for the time-dependent mode field operators $\hat{a}_{\lambda}(t)$:

$$i\hbar \frac{d\hat{a}_{\lambda}(t)}{dt} = [\hat{a}_{\lambda}(t), \hat{H}(t)], \quad (3)$$

where $\hat{H}(t)$ is the Hamiltonian of the system. For the usual general types of interaction of the field with matter, including the interaction of light with a

random medium,⁹ these equations may be solved in the form¹¹

$$\hat{a}_\lambda(t) = \sum_\mu [u_{\lambda\mu}(t) \hat{a}_\mu + v_{\lambda\mu}(t) \hat{a}_\mu^\dagger], \quad (4)$$

where the functions $u_{\lambda\mu}(t)$ and $v_{\lambda\mu}(t)$ are obtained in the process of solving Eq. (3), and \hat{a}_λ and \hat{a}_λ^\dagger are the initial values of the annihilation and creation operators, respectively; these functions obey the identities

$$uu^\dagger - vv^\dagger = 1, \quad (5a)$$

$$u\bar{v} - v\bar{u} = 0 \quad (5b)$$

as a consequence of the validity of the commutation rules

$$[\hat{a}_\lambda(t), \hat{a}_{\lambda'}^\dagger(t)] = [\hat{a}_\lambda, \hat{a}_{\lambda'}^\dagger] = \delta_{\lambda\lambda'}, \quad (6a)$$

$$[\hat{a}_\lambda(t), \hat{a}_{\lambda'}(t)] = [\hat{a}_\lambda^\dagger(t), \hat{a}_{\lambda'}^\dagger(t)] = 0, \quad (6b)$$

In Eqs. (5), u^\dagger and v^\dagger are the Hermitian conjugates to the matrices u and v , while \bar{u} and \bar{v} are their transposes. For our purposes it is sufficient to consider only the diagonal elements of the matrices u and v , while off-diagonal elements may be neglected¹⁰; we denote $u_{\lambda\lambda} \equiv u_\lambda$ and $v_{\lambda\lambda} \equiv v_\lambda$. This assumption implies that permittivity fluctuations of the random medium vary slowly with the spatial variable \vec{x} . Thus Eq. (5b) reduces to the trivial identity, and Eq. (5a) yields

$$|u_\lambda|^2 - |v_\lambda|^2 = 1. \quad (7)$$

For the case of radiation transmitted through the turbulent atmosphere or other random media, however, we may assume the medium to be passive and therefore we may neglect the second term in Eq. (4) and write^{9,10}

$$\hat{a}_\lambda(t) \approx u_\lambda(t) \hat{a}_\lambda. \quad (8)$$

This approximation implies that the self-radiation of the medium is not taken into account. Although Eq. (8) violates the commutation rules [Eqs. (6)] in the exact sense, we may assume that they are valid for $\hat{a}_\lambda(t)$ in the approximate sense.

We define the normal characteristic function (see, e.g., Ref. 12) by

$$\begin{aligned} C^{(N)}(\{\beta_\lambda\}, t) &= \text{Tr} \left\{ \hat{\rho}(t) \prod_\lambda e^{\beta_\lambda \hat{a}_\lambda^\dagger} e^{-\beta_\lambda^* \hat{a}_\lambda} \right\} \\ &= \text{Tr} \left\{ \hat{\rho} \prod_\lambda e^{\beta_\lambda \hat{a}_\lambda^\dagger(t)} e^{-\beta_\lambda^* \hat{a}_\lambda(t)} \right\}, \end{aligned} \quad (9a)$$

and the photon-number characteristic function by

$$C^{(n)}(is, t) = \text{Tr} \{ \hat{\rho}(t) e^{is \hat{n}} \} = \text{Tr} \{ \hat{\rho} e^{is \hat{n}(t)} \}, \quad (9b)$$

where β_λ are complex numbers, s is a parameter, \hat{n} is given by Eq. (1), $\hat{\rho}$ is the density matrix in-

dependent of t in the Heisenberg picture, and $\hat{\rho}(t)$ is the time-dependent density matrix in the Schrödinger picture. Moreover, making use of the Glauber-Sudarshan diagonal representation for the density matrix^{13,14}

$$\hat{\rho}(t) = \int \phi(\{\alpha_\lambda\}, t) |\{\alpha_\lambda\}\rangle \langle \{\alpha_\lambda\}| d^2\{\alpha_\lambda\} \quad (10)$$

[here $|\{\alpha_\lambda\}\rangle$ represents a coherent state, while $\phi(\{\alpha_\lambda\}, t)$ is a weight function], we obtain from Eq. (9a) (see Ref. 14) that

$$\begin{aligned} \phi(\{\alpha_\lambda\}, t) &= \int C^{(N)}(\{\beta_\lambda\}, t) \\ &\times \prod_\lambda \exp(-\beta_\lambda \alpha_\lambda^* + \beta_\lambda^* \alpha_\lambda) d^2\beta_\lambda / \pi^2, \end{aligned} \quad (11)$$

while the integrated intensity distribution $P(W, t)$ is given by

$$P(W, t) = \int \phi(\{\alpha_\lambda\}, t) \delta\left(W - \sum_\lambda |\alpha_\lambda|^2\right) d^2\{\alpha_\lambda\}. \quad (12)$$

Using Eqs. (9a) and (8) in Eq. (11), we arrive at

$$\begin{aligned} \phi(\{\alpha_\lambda\}, t) &= \int \phi(\{\gamma_\lambda\}, 0) \prod_\lambda \delta(\alpha_\lambda - u_\lambda(t) \gamma_\lambda) d^2\gamma_\lambda \\ &= \left\langle \prod_\lambda \delta(\alpha_\lambda - u_\lambda(t) \gamma_\lambda) \right\rangle, \end{aligned} \quad (13)$$

where we have used Eq. (10) for $t=0$; γ_λ is the eigenvalue of \hat{a}_λ in the coherent state $|\{\gamma_\lambda\}\rangle$. From Eq. (13) it is clear that the initially coherent state remains coherent for all time. Further substitution of Eq. (13) into Eq. (12) yields the expression

$$P(W, t) = \left\langle \delta\left(W - \sum_\lambda |u_\lambda(t)|^2 |\gamma_\lambda|^2\right) \right\rangle. \quad (14a)$$

We further assume that all $u_\lambda(t)$ are the same,¹⁰ i.e., all mode functions are very closed and various modes are specified by the wave vectors $\vec{k}_1, \vec{k}_2, \dots$, with $|\vec{k}_1| = |\vec{k}_2| = \dots$. Denoting $|u_\lambda(t)|^2 \equiv K(t)$, which is the typical fluctuating quantity in the random medium obeying the log-normal probability distribution in the turbulent atmosphere, and also denoting $W_0 = \sum_\lambda |\gamma_\lambda|^2$, we may rewrite Eq. (14a) in the form

$$P(W, t) = \langle \delta(W - K(t) W_0) \rangle. \quad (14b)$$

Assuming unity photoefficiency for simplicity, the photon counting distribution is then given by

$$\begin{aligned} p(n) &\equiv p(n, t) = \int_0^\infty P(W, t) (W^n / n!) e^{-W} dW \\ &= \int_0^\infty \int_0^\infty P(W_0) \bar{P}(K) \delta(W - KW_0) \\ &\quad \times (W^n / n!) e^{-W} dW_0 dK dW \\ &= \int_0^\infty \int_0^\infty P(W_0) \bar{P}(K) [(KW_0)^n / n!] e^{-KW_0} dW_0 dK \\ &= \int_0^\infty p_0(n, K \langle n \rangle) \bar{P}(K) dK, \end{aligned} \quad (15)$$

where the additional average over K with the probability distribution $\bar{P}(K)$ has been carried out, and

$$p_0(n, K\langle n \rangle) = \int_0^\infty P(W_0) [(KW_0)^n / n!] e^{-KW_0} dW_0. \quad (16)$$

Equation (16) represents the counting distribution for radiation in the absence of atmosphere. In Eq. (15), the total mean photon number $\langle n \rangle$ is assumed to be a stochastic quantity $K\langle n \rangle$. This is just the description proposed by Diamant and Teich.¹ In general, the distribution $\bar{P}(K)$ depends on the time $t = z/c$, where z is the traveled distance.

We return now to Eq. (9b). Substituting $\hat{n}(t) = \sum_\lambda \hat{a}_\lambda^\dagger(t) \hat{a}_\lambda(t)$ into Eq. (9b) and using Eqs. (6), we obtain (see, e.g., Ref. 14) the following photon-number characteristic function:

$$C^{(n)}(is, t) = \langle \exp[is\hat{n}(t)] \rangle = \mathfrak{N} \exp[(e^{is} - 1)\hat{n}(t)] \\ = \langle \exp[(e^{is} - 1)W(t)] \rangle. \quad (17)$$

Here \mathfrak{N} denotes the normal order of the operator. Equations (8) and (10) for $t=0$ have been used, as has the expression

$$W(t) = \langle \{ \alpha_\lambda \} | \hat{n}(t) | \{ \alpha_\lambda \} \rangle = \sum_\lambda | \alpha_\lambda(t) |^2 = K(t) W_0.$$

Note that

$$K(t) \equiv |u_{\lambda,}(t)|^2,$$

$$W_0 = \langle \{ \alpha_\lambda \} | \hat{n}_0 | \{ \alpha_\lambda \} \rangle = \sum_\lambda | \alpha_\lambda |^2, \quad \hat{n}_0 = \sum_\lambda \hat{a}_\lambda^\dagger \hat{a}_\lambda.$$

A Fourier transform of Eq. (17) leads to Eq. (15) again [under the brackets in Eqs. (17) and (18) we understand that the average is also over K].

On the other hand, using Eqs. (6) and (8), we may write

$$C^{(n)}(is, t) = \langle \exp[is\hat{n}(t)] \rangle = \langle \exp[isK(t)\hat{n}_0] \rangle \\ = \langle \exp[(e^{isK(t)} - 1)W_0] \rangle. \quad (18)$$

A Fourier transform of this quantity yields precisely the modified photodetection equation obtained in Ref. 8 as a consequence of the Tatarski description:

$$p(\nu) \equiv p(\nu, t) = p_0(0) \delta(\nu) + \sum_{n=1}^{\infty} \frac{p_0(n) \bar{P}(\nu/n)}{n}. \quad (19)$$

We have used ν instead of n to point out that $n(t)$ in Eq. (18) is not an integer [which is a consequence of the fact that $K(t)$ is not integer]; $\delta(\nu)$ is the Dirac δ function. It is clear that $\int_0^\infty p(\nu) d\nu = 1$, and for $\sigma \rightarrow 0$ [in Eq. (20)] it holds that $p(\nu) = p_0(\nu)$. For the case of the turbulent atmosphere, the probability distribution $\bar{P}(K)$ is given by the log-normal distribution¹

$$\bar{P}(K) = \frac{1}{(\sqrt{2\pi})\sigma K} \exp\left(-\frac{(\ln K + \frac{1}{2}\sigma^2)^2}{2\sigma^2}\right), \quad (20)$$

where σ is the standard deviation of the logarithm of K .

We see that Eq. (19) represents a generalized function arising as a result of the rapid growth of the corresponding sth moment,

$$\langle \nu^s \rangle = \langle K^s \rangle \sum_{j=1}^s a_j \langle W_0^j \rangle, \quad (21a)$$

while from Eq. (15)

$$\langle n^s \rangle = \sum_{j=1}^s a_j \langle K^j \rangle \langle W_0^j \rangle, \quad (21b)$$

where the a_j are well-known coefficients (see, e.g., Ref. 14). Thus, in the Tatarski description, the influence of the random medium is included in the photon number ν [$\nu(t) = K(t)\hat{n}_0$], while in the Diamant-Teich description, it is included in the "classical" integrated intensity [$W(t) = K(t)W_0$].⁸ Consequently, the Tatarski description includes the physical vacuum of the self-radiation of the medium, while this radiation is completely neglect-

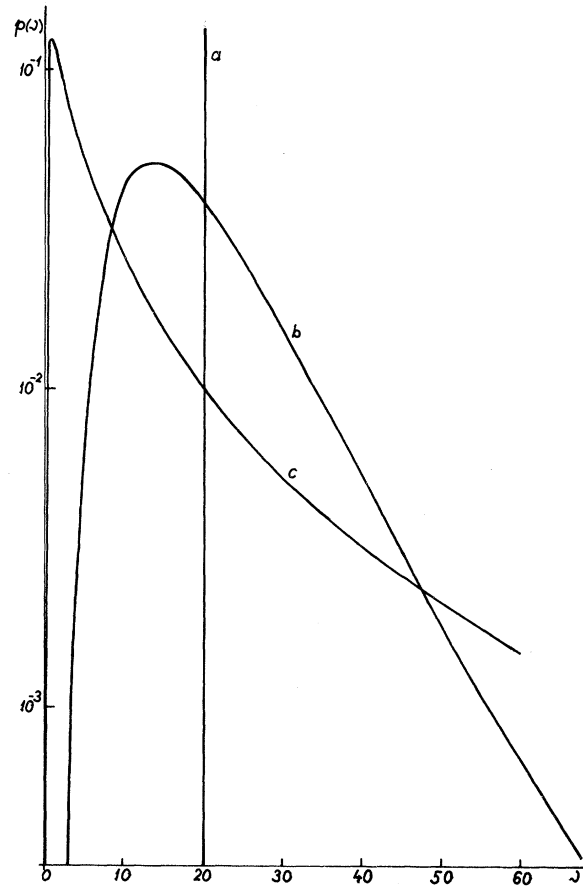


FIG. 1. The photon counting distribution $p(\nu)$ vs ν for the levels of turbulence $\sigma=0$ (line a), $\sigma=\frac{1}{2}$ (curve b), and $\sigma=\frac{3}{2}$ (curve c) for an incident field in the Fock state $|20\rangle$. Both the Diamant-Teich and the Tatarski descriptions give the same result.

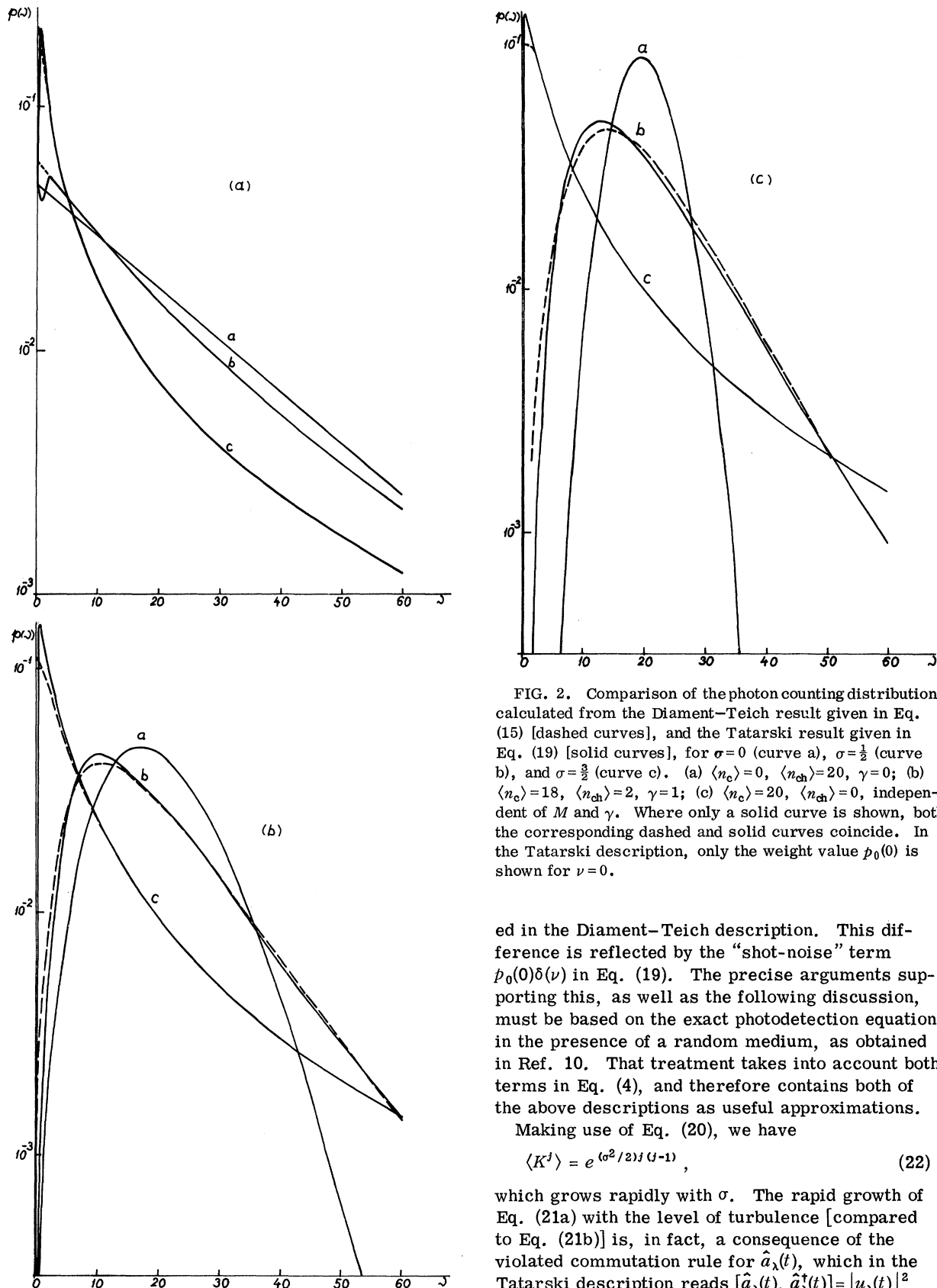


FIG. 2. Comparison of the photon counting distributions calculated from the Diamant-Teich result given in Eq. (15) [dashed curves], and the Tatarski result given in Eq. (19) [solid curves], for $\sigma=0$ (curve a), $\sigma=\frac{1}{2}$ (curve b), and $\sigma=\frac{3}{2}$ (curve c). (a) $\langle n_c \rangle=0$, $\langle n_{ch} \rangle=20$, $\gamma=0$; (b) $\langle n_c \rangle=18$, $\langle n_{ch} \rangle=2$, $\gamma=1$; (c) $\langle n_c \rangle=20$, $\langle n_{ch} \rangle=0$, independent of M and γ . Where only a solid curve is shown, both the corresponding dashed and solid curves coincide. In the Tatarski description, only the weight value $p_0(0)$ is shown for $\nu=0$.

ed in the Diamant-Teich description. This difference is reflected by the "shot-noise" term $p_0(0)\delta(\nu)$ in Eq. (19). The precise arguments supporting this, as well as the following discussion, must be based on the exact photodetection equation in the presence of a random medium, as obtained in Ref. 10. That treatment takes into account both terms in Eq. (4), and therefore contains both of the above descriptions as useful approximations.

Making use of Eq. (20), we have

$$\langle K^j \rangle = e^{(\sigma^2/2)j(j-1)}, \quad (22)$$

which grows rapidly with σ . The rapid growth of Eq. (21a) with the level of turbulence [compared to Eq. (21b)] is, in fact, a consequence of the violated commutation rule for $\hat{a}_\lambda(t)$, which in the Tatarski description reads $[\hat{a}_\lambda(t), \hat{a}_\lambda^\dagger(t)] = |u_\lambda(t)|^2$

$\equiv K(t) \geq 1$ [from Eq. (7)]. However, the commutator reflects the contribution of the physical vacuum, and so this leads to an increase of the probability of observing the vacuum state ($\nu = 0$), where the difference between Eqs. (21a) and (21b) is cumulated. We see from Eq. (19) that for $\nu = 0$ only the first singular term [if $p_0(0) \neq 0$] is nonzero if $\bar{P}(K)$ is given by Eq. (20), while for $\nu > 0$ the first term equals zero, and only the second regular term in Eq. (19) is nonzero. The probability of observing a nonzero number of photons (photoelectrons) is altered very little compared to Eq. (15). This is demonstrated for various states of the field by the numerical data presented in Sec. III.

III. NUMERICAL COMPARISON OF THE TWO DESCRIPTIONS

First we discuss the Fock state $|m\rangle$ for which $p_0(n) = \delta(n - m)$; in this case Eq. (19) gives

$$p(\nu) = \frac{\bar{P}(\nu/m)}{m}$$

[$p_0(0) = 0$ for $m > 0$], while Eq. (15) leads to the same expression,

$$p(n) = \int_0^\infty \delta(n - Km) \bar{P}(K) dK = \frac{\bar{P}(n/m)}{m},$$

using the property for the Dirac δ function $a\delta(ax) = \delta(x)$, for $a > 0$. The corresponding curves are presented in Fig. 1 for $\sigma = 0, \frac{1}{2}$, and $\frac{3}{2}$ (the highest value corresponds to the very turbulent atmosphere), demonstrating the influence of turbulence on the photon counting distribution in a "pure" form.

Next we have numerically compared the two prescriptions, Eqs. (15) and (19), for incident chaotic light, coherent light, and their superposition. For $p_0(n)$, we have used the physically realistic expression^{15,16}

$$p_0(n) = \frac{1}{\Gamma(n+M)} \left(1 + \frac{\langle n_{ch} \rangle}{M}\right)^{-M} \left(1 + \frac{M}{\langle n_{ch} \rangle}\right)^{-n} \times \exp \left[-\frac{\langle n_c \rangle M}{\langle n_{ch} \rangle + M} \right] L_n^{M-1} \left(-\frac{\langle n_c \rangle M^2}{\langle n_{ch} \rangle (\langle n_{ch} \rangle + M)} \right), \quad (23)$$

where $\Gamma(z)$ is the gamma function, $L_n^M(z)$ are the Laguerre polynomials,¹⁷ $\langle n_c \rangle$ and $\langle n_{ch} \rangle$ are the mean photon numbers in the coherent and chaotic fields, respectively, and the degrees-of-freedom parameter M is given by¹⁸⁻²⁰

$$M = \frac{\langle n_{ch} \rangle + 2\langle n_c \rangle}{\langle n_{ch} \rangle y_1 + 2\langle n_c \rangle \bar{y}_1}, \quad (24)$$

with

$$y_1 = T^{-2} \int_0^T \int_0^T |\gamma^{ch}(t_1 - t_2)|^2 dt_1 dt_2, \quad (25a)$$

and

$$\bar{y}_1 = T^{-2} \operatorname{Re} \int_0^T \int_0^T \gamma^{ch}(t_1 - t_2) \gamma^c(t_2 - t_1) dt_1 dt_2. \quad (25b)$$

Here γ^c and γ^{ch} are the second-order degrees of coherence for coherent and chaotic fields, respectively. We have performed the calculations for a Lorentzian spectrum with chaotic light of mean frequency ω_0 in coincidence with coherent light of frequency ω_c ⁶ for $\langle n_c \rangle = 0$, $\langle n_{ch} \rangle = 20$ (pure chaotic light); $\langle n_c \rangle = 18$, $\langle n_{ch} \rangle = 2$ (superposition of coherent and chaotic light); $\langle n_c \rangle = 20$, $\langle n_{ch} \rangle = 0$ (pure coherent light); and for $\gamma = \Gamma T = 0$ (0.01), 1, and 100 (Γ is the half-width of the spectrum), with $\sigma = 0, \frac{1}{2}$, and $\frac{3}{2}$. The data calculated from Eq. (15) have been discussed in Ref. 6, while those obtained from Eq. (19) have been calculated using the Columbia University IBM 360/91 computer. The influence of the turbulent atmosphere on the photon counting distribution has been discussed in Refs. 1-3, and for light of arbitrary spectrum in Ref. 6; it has been shown that turbulence leads to shifts of the maxima of the photon counting distributions to lower values of ν and to a broadening of the curves (cf. Fig. 1). It also leads to a smoothing of spectral information (with increasing $\gamma = \Gamma T$, all curves tend to peak).

Consequently, we compare only the values obtained with the help of both methods for $\sigma = 0, \frac{1}{2}$, and $\frac{3}{2}$ (curves a, b, c) and for $\langle n_c \rangle = 0$, $\langle n_{ch} \rangle = 20$, $\gamma = 0$ [Fig. 2(a)]; $\langle n_c \rangle = 18$, $\langle n_{ch} \rangle = 2$, $\gamma = 1$ [Fig. 2(b)]; and $\langle n_c \rangle = 20$, $\langle n_{ch} \rangle = 0$, independent of M and γ [Fig. 2(c)]. The solid curves are calculated after Eq. (19), while the dashed curves are calculated after Eq. (15). If only one curve is shown, the corresponding dashed and solid curves coincide. In the Tatarski description, we show the weight value $p_0(0)$ for $\nu = 0$ [instead of $p_0(0)\delta(0)$]. As may be seen from the figures, there is good agreement for both descriptions when $\nu > 0$; similar agreement occurs for all other values of parameters not displayed here. Of course, for $\sigma = 0$, the descriptions precisely coincide.

Finally, we note that although both descriptions are identical for the Fock state $|m\rangle$, they differ from one another for the vacuum state $|0\rangle$, where $p(\nu) = p_0(0)\delta(\nu)$ in the Tatarski description, and where $p(n) = p_0(0)$ for $n = 0$ and $p(n) = 0$ for $n > 0$ in the Diamant-Teich description. Thus the difference between the descriptions is cumulated in $\delta(\nu)$.

*Work supported by the National Science Foundation.

¹P. Diamant and M. C. Teich, J. Opt. Soc. Am. **60**, 1489 (1970).

²P. Diamant and M. C. Teich, Appl. Opt. **10**, 1664 (1971).

³M. C. Teich and S. Rosenberg, Opto-Electron. **3**, 63 (1971).

⁴R. Y. Yen, P. Diamant, and M. C. Teich, IEEE Trans. Inf.

Theory IT-18, 302 (1972).

⁵S. Rosenberg and M. C. Teich, J. Appl. Phys. **43**, 1256 (1972).

⁶J. Peřina and V. Peřinová, Czech. J. Phys. B **22**, 1085 (1972).

⁷V. I. Tatarski, Zh. Eksp. Teor. Fiz. **61**, 1822 (1971) [Sov. Phys.-JETP **34**, 969 (1972)].

⁸J. Peřina, Czech. J. Phys. B **22**, 1075 (1972).

⁹B. Crosignani, P. Di Porto, and S. Solimeno, Phys. Rev. D **3**, 1729 (1971).

¹⁰J. Peřina, V. Peřinová, and R. Horák, Czech. J. Phys. B (to be published).

¹¹B. R. Mollow, Phys. Rev. **162**, 1256 (1967).

¹²B. R. Mollow and R. J. Glauber, Phys. Rev. **160**, 1076 (1967).

¹³J. R. Klauder and E. C. G. Sudarshan, *Fundamentals of Quantum Optics* (Benjamin, New York, 1968).

¹⁴J. Peřina, *Coherence of Light* (Van Nostrand, London, 1972).

¹⁵J. Peřina, Phys. Lett. **24A**, 333 (1967).

¹⁶J. Peřina and R. Horák, J. Phys. A **2**, 702 (1969).

¹⁷P. M. Morse and H. Feshbach, *Methods of Theoretical Physics* (McGraw-Hill, New York, 1953), Vol. I.

¹⁸R. Horák, L. Miřta, and J. Peřina, J. Phys. A **4**, 231 (1971).

¹⁹R. Horák, L. Miřta, and J. Peřina, Czech. J. Phys. B **21**, 614 (1971).

²⁰J. Peřina, V. Peřinová, and L. Miřta, Opt. Commun. **3**, 89 (1971).

Calculation of the Structure and Energy of Nematic Threads

Jürgen Nehring

Brown Boveri Research Center, CH-5401 Baden, Switzerland

(Received 21 November 1972)

Continuum theory is used to calculate the molecular alignment and the elastic deformation energy in a nematic layer containing a circular-loop thread. In agreement with experiment, planar solutions are found, with the thread being the boundary between regions of different pitch. It is shown that threads in nematics and Grandjean lines in cholesterics are equivalent-alignment structures and that a thread located in the midplane of the layer is in equilibrium with respect to displacements normal to the layer. From an analogy to the case of magnetic fields general conclusions are drawn as to the alignment near threads of general shape outside the core. A model of a nonsingular core is given for threads of type $|s|=1$ and the alignment near point singularities is calculated.

I. INTRODUCTION

Nematic liquid crystals are named after the threadlike structures often observed in this type of liquid crystal.¹ With some materials, nematic threads may be generated in plane layers with defined boundary alignment by use of electric fields.^{2,3} Two examples of threaded textures as obtained in this manner are shown in Figs. 1(a) and 1(b). The boundary alignment was the same on both surfaces and perpendicular to the layer normal. Polarized light was used for observation, the direction of polarization being perpendicular to the surface alignment for Fig. 1(a) and parallel for Fig. 1(b). Two types of threads may be distinguished. The first type appears as a narrow black line for both directions of polarization of the incoming light. The width of the black lines, which may be called the core diameter of the thread, is of the order of 1 μm and is independent of sample thickness, as was found for thicknesses ranging from 40 to 250 μm . The black line originates from light scattering at the core. The second type of thread has a more extended core as seen in Fig. 1(a), with the core diameter being approximately $d/10$, where d is the sample thickness. This type of thread is surrounded by a dark shadow of width $d/2$ when observed with light polarized parallel to the surface

alignment [Fig. 1(b)]. The shadow is caused by a deviation from the planar orientation⁵ that is observed everywhere else in the sample. Another indication of deviation from planar orientation in the case of a thick thread is the occurrence of point singularities,³ two of which are seen in Fig. 1(b). While in Fig. 1 threads of the first type ("thin threads") separate regions without twist from twisted regions of pitch $|P|=2d$, threads of the second type ("thick threads") separate regions of pitch $P=2d$ from those of pitch $P=-2d$.³ Thin threads generally form closed loops whereas thick threads may be attached by their ends to a thin one. Threads are mostly located in the midplane of the sample but deviations from this arrangement are sometimes observed. A thread may be several millimeters long and the area surrounded by a closed thread may have any shape. It is however often observed that when a closed thread shrinks it approaches a circular shape [Figs. 2(a) and 2(b)].

In the following, alignment and energy of a sample containing a single circular-loop thread will be calculated assuming isotropic elasticity and planar orientation. In addition, it will be shown that some general conclusions can be drawn as to the alignment near threads of more general shape. Nonplanar solutions of the equilibrium equations